First-principles study of native defects in anatase TiO_2

Sutassana Na-Phattalung,[1,2] M. F. Smith,[1] Kwiseon Kim,[3] Mao-Hua Du,[3] Su-Huai Wei,[3]
S. B. Zhang,[3] and Sukit Limpijumnong[1,2,3]
[1]*National Synchrotron Research Center, Nakhon Ratchasima, Thailand*
[2]*School of Physics, Suranaree University of Technology, Nakhon Ratchasima, Thailand*
[3]*National Renewable Energy Laboratory, Golden, Colorado 80401, USA*
(Received 21 January 2006; revised manuscript received 27 February 2006; published 31 March 2006)

Native point defects in anatase TiO_2 are investigated by using first-principles pseudopotential calculations based on density-functional theory (DFT). Antisite defects, namely, Ti-antisite (Ti_O) and O-antisite (O_{Ti}), have high formation energies and are hence unstable. In contrast, all other fundamental native defects (Ti_i, O_i, V_{Ti}, and V_O) have low formation energies. In particular, titanium interstitial (Ti_i) is a quadruple donor defect with lowest formation energy in *p*-type samples, whereas Ti vacancy (V_{Ti}) is a quadruple acceptor defect with lowest formation energy in *n*-type samples. Interstitial oxygen (O_i) would spontaneously and strongly bind to lattice oxygen, resulting in a neutral O_2 dimer substituting on one O site. None of the four low-energy defects have energy levels inside the DFT band gap.

DOI: 10.1103/PhysRevB.73.125205 PACS number(s): 61.72.Bb, 61.72.Ji

I. INTRODUCTION

Semiconductor photocatalysis begins with the activation of an electron from the valence band to the conduction band by optical excitation, creating an electron in the conduction band and a hole in the valence band. These excited carriers may diffuse to the surface to initiate chemical reactions with agents in the surrounding fluid. (The process is commonly applied to air and water purification, for which the relevant chemical reactions are those resulting in the destruction of various microorganisms.[1,2]) Electron-hole recombination is an important competing process, as it tends to prevent the carriers from reaching the surface. The efficiency of a photocatalytic process involving visible light thus depends mainly on two factors: (i) the absorption of the semiconductor in the visible region, which determines the initial number of carriers being created, and (ii) the time required for the excited carrier to move to the surface to initiate reactions, as compared to the recombination lifetime. The ratio between these two time constants determines the fraction of the carriers that will take part in photocatalysis. In this regard, it is often beneficial to use small particles ranging between 1 and 100 nm in diameter to maximize the photocatalytic rates.

TiO_2 has been successfully applied as a semiconductor photocatalyst. Its main advantages over similar materials are its high oxidizing power and durability (i.e., high resistance to photo- and chemical corrosion). A major drawback of the TiO_2, however, is its large band gap, which does not permit efficient absorption of visible light and hence prevents TiO_2 from being used in large-scale environmental applications. There is a rich literature describing the attempts to chemically dope TiO_2 in order to reduce the band gap, but how to best manipulate the gap while maintaining the beneficial photocatalytic properties is still an unresolved challenge. For example, one of the difficulties in the chemical doping is that, while reducing the band gap, the dopants also act as carrier scattering centers and traps, which reduce the chance for the carriers to reach particle surfaces to participate in the desired reactions. Further complications arise in an effort to distinguish the effect of surface impurities from that of bulk impurities.

These problems underscore the need to understand, in detail, the changes in TiO_2 that result from impurity introduction. Before this can be done, however, one also has to understand the role of native defects in TiO_2. Native defects could influence both of the factors mentioned above. The concentration of the native defects typically depends on the growth conditions, as well as on the presence of chemical impurities. This implies that it will be difficult for an experimentalist to unravel the effect of a particular chemical impurity simply from measuring the doping dependence of a photocatalytic process, because it is difficult to get rid of all the native defects. It is therefore desirable to study the properties of the defects. At the very least, one should know what can be expected under the various growth conditions, so that the experimental results can be interpreted without any ambiguity arising from the contribution of the native defects.

TiO_2 has three polymorphs: rutile, anatase, and brookite. Rutile TiO_2 is the most studied phase. This is probably due to its simple crystal structure and to the fact that rutile single crystal, as well as thin film, can be readily grown by several conventional techniques. Brookite TiO_2 is the least studied TiO_2, due to its complex structure and naturally the difficulties encountered during growth. Although bulk single-crystal anatase is less stable than bulk rutile, nanoparticles of TiO_2 used in photocatalysis and photoelectrochemistry[3] tend to exhibit only the anatase structure. For this reason, we will consider here the anatase polymorph. To our knowledge, no first-principles studies of native point defects in any form of the TiO_2 have previously been carried out.

Using first-principles total-energy calculations, we have investigated the fundamental native point defects in anatase TiO_2. These include Ti vacancy (V_{Ti}), O vacancy (V_O), Ti interstitial (Ti_i), and O interstitial (O_i). All can have very low, and even negative, formation energies depending on the growth conditions. We have also studied the antisites and found that they have very high energies due to the large

TABLE I. Formation energy of native defects in anatase TiO_2 with the Fermi level at the VBM. The results are shown for both the 48- and 108-atom supercells. Both the Ti-rich ($\mu_{Ti}=-2.67$ eV, *precipitated by* Ti_2O_3; $\mu_O=-3.79$ eV) and O-rich ($\mu_{Ti}=-10.25$ eV; $\mu_O=0$ eV) conditions are shown.

		E_f (eV) (Ti-rich[a])		E_f (eV) (O-rich)	
Defect	Charge state	48-atom	108-atom	48-atom	108-atom
Ti_i	+4	−9.88	−9.42	−2.31	−1.84
V_{Ti}	−4	12.64	13.40	5.06	5.82
$O_i \equiv (O_2)_O$	0	4.50	4.40	0.71	0.61
V_O	+2	−2.82	−3.26	0.97	0.52
O_{Ti}	−4		21.91		10.54
Ti_O	+6		−6.83		4.53

[a]For the Ti-rich case, we have taken into account the formation of Ti_2O_3, which has a lower energy than the Ti metal.

cation-anion size mismatch and strong ionicity of TiO_2 (see Table I). The formation energy of an antisite is even higher than the sum of those for vacancy and interstitial. For instance, the energy of O_{Ti} is higher than the sum of V_{Ti} and O_i. This means O_{Ti} is unstable against spontaneous disintegration into a pair of isolated V_{Ti} and O_i. Since antisites are unlikely to form in TiO_2, they are excluded from the discussion below. Due to a strong preference of the interstitial O_i to bind strongly with lattice O, however, a substitutional diatomic molecule (O_2) always forms on the O site. To be consistent with our earlier work of defects in ZnO, we will call this paired oxygen $(O_2)_O$.[4]

Interestingly, none of the above defects has a level inside the density functional theory (DFT) band gap. This finding is unexpected because, typically, native defects in wide gap semiconductors[5–7] do introduce deep levels inside the DFT gaps. Later in the paper we will present a simple qualitative picture to show why the more ionic TiO_2 is distinct from other semiconductors in this way.

II. COMPUTATIONAL METHOD

We used the DFT with the local density approximation (LDA) and ultrasoft pseudopotentials,[8] as implemented in the VASP codes.[9] The cutoff energy for the plane-wave basis set is 300 eV. Our calculated crystal parameters of bulk anatase TiO_2 are $a=3.764$, $c/a=2.515$, and $u=0.208$. These are in good agreement with the experimental values: $a=3.785$, $c/a=2.513$, and $u=0.208$ (Ref. 10). Other calculations[11–13] showed similar agreement. To calculate the formation energy of the defects, a supercell approach is used[14,15] in which all atoms are allowed to relax by minimization of the Hellmann-Feynman force to less than 0.05 eV/Å. Our preliminary study was based on a supercell with 48 atoms, as a $2\times2\times2$ repetition of the primitive anatase unit cell. To ensure the convergence of the calculations, especially for high charge-state defects, we repeated all the calculations with a larger supercell size of 108 atoms (namely $3\times3\times2$). We found that formation energies calculated using the 48-atom cell typically agree to within 0.45 eV with those calculated using the 108-atom cell [best case: $(O_2)^0_O$, 0.1 eV; worst case: V^{4-}_{Ti}, 0.76 eV]. For the Brillouin zone integration, a $2\times2\times2$ Monkhorst-Pack special k-point mesh is used regardless of the cell size. Unless noted otherwise, all results presented here are based on the 108-atom cell calculations. We will present the electronic structure using a special k-point scheme as discussed in Ref. 16. The calculated band gap averaged over the special k is 2.32 eV. Due to the well-known LDA gap error, the calculated band gap is smaller than the experimental band gap of 3.2 eV.[17]

For a supercell, the defect formation energy is defined as[14]

$$E_f = E_{tot}(D^q) - E_{tot}(0) + \sum \Delta n_x \mu_x + qE_f, \quad (1)$$

where $E_{tot}(D^q)$ is the total energy of the cell with defect D in charge state q. $E_{tot}(0)$ is the total energy of the cell without the defect and Δn_X is the number of atoms from species X (=Ti, O) being removed from a defect-free cell, to its respective reservoir with chemical potential μ_X, to form the defect cell. The chemical potential reflects the availability (or elemental partial pressure) of each element. During the growth, if any chemical potential rises above its natural phase value (i.e., that of hcp Ti and O_2 molecule), then the natural phase will form instead of the TiO_2. Because of this, only the μ_X values below those of the natural phases need to be considered. More strict limitations on the chemical potentials may be imposed by the formation of alternative phases containing both Ti and O, as will be discussed below.

If the TiO_2 crystal is to grow slowly, it is required that

$$\mu_{TiO_2} = \mu_{Ti} + 2\mu_O, \quad (2)$$

where μ_{TiO_2} is the chemical potential of anatase TiO_2. If we set $\mu_X=0$ for their respective natural phases, then $\mu_{TiO_2}=-10.25$ eV is the calculated formation energy of anatase TiO_2 per molecular formula. The constraint, Eq. (2), ensures equilibrium growth conditions. If the sum on the right-hand side is larger than μ_{TiO_2}, then the crystal will grow rapidly and will not be homogeneous. On the other hand, if this sum is lower than μ_{TiO_2}, then the crystal will disintegrate instead of grow.

In Fig. 1, we illustrate the allowable conditions of growth on a graph of μ_{Ti} versus μ_O. The condition given by Eq. (2) is indicated by a solid line. There are other titanium-oxygen stable phases that may exist, including Ti_2O_3 and TiO. Since the Ti-to-O ratio is higher in both Ti_2O_3 and TiO than that in TiO_2, we expect the growth of these alternate phases to be favorable under the Ti-rich growth conditions. To determine whether the formation of these alternative phases imposes a stricter upper limit on μ_{Ti}, we need to consider the equilibrium growth of Ti_2O_3 and TiO. For example for Ti_2O_3, equilibrium growth takes place when

$$\mu_{Ti_2O_3} = 2\mu_{Ti} + 3\mu_O, \quad (3)$$

where $\mu_{Ti_2O_3}=-16.7$ eV is the calculated formation energy of Ti_2O_3. Equation (3) (and the corresponding expression for TiO) is illustrated by a dashed (and dotted) line in Fig. 1. We see that the lines corresponding to Eqs. (2) and (3) intersect

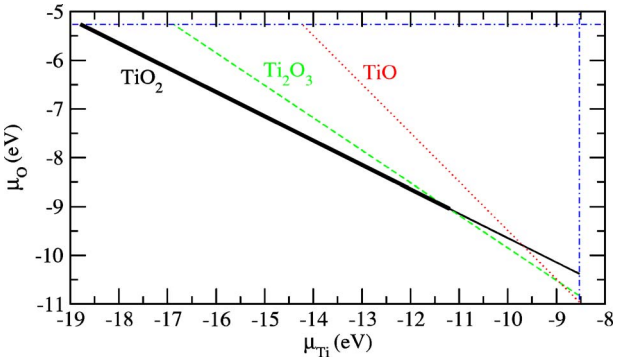

FIG. 1. (Color online) Graphic illustration of thermodynamic growth conditions for TiO_2, i.e., the allowed values of the atomic chemical potentials, μ_{Ti} and μ_O. The dot-dashed horizontal and vertical lines indicate the upper bounds determined by the natural phases of Ti and O, respectively. Equilibrium growth of TiO_2 takes place for μ_{Ti} and μ_O lying on the solid line, whereas equilibrium growth of Ti_2O_3 and TiO takes place for μ_{Ti} and μ_O lying in the dashed and dotted lines, respectively.

at $\mu_{Ti}=-2.67$ eV. For higher values of μ_{Ti}, the growth of Ti_2O_3 is expected to proceed much more rapidly than that of TiO_2, so that we may regard $\mu_{Ti}=-2.67$ eV as the real upper limit for the TiO_2 growth. With this, the range of allowable growth conditions is described by the bold solid line in Fig. 1.

In our calculations, we vary the charge of the defect in order to identify the most stable charge state. To calculate the charged defects, a jellium background is used to neutralize the supercell. We have not applied any correction to the fictitious electrostatic interactions between the charged defect and its images in the neighboring supercells. This is justifiable especially in the case of TiO_2 where the dielectric constant ($\varepsilon > 100$) (Ref. 18) is about an order of magnitude higher than other semiconductors. The high dielectric constant results in small correction terms for the fictitious electrostatic interactions. For instance, the leading term of the Makov-Payne correction[19] for the charge state 4± in the 108-atom cell is only about 0.1 eV, which is comparable to the expected error bars of our calculations. Moreover, we compare the results of the 48- and 108-atom cells to estimate the errors arising from the finite cell size and the supercell shape.

The concentration of a defect (c) is related to its formation energy E_f through the equation

$$c = N_{\text{sites}} \exp(-E_f/kT), \tag{4}$$

where N_{sites} is the number of possible lattice sites per unit volume to form the defect, k is Boltzmann's constant, and T is the temperature in Kelvin. To be exact, Eq. (4) is only valid under thermodynamic equilibrium. Regardless of whether the growth/anneal process is under the thermal equilibrium or not, the formation energy is still a good indicator of the abundance of the defect: namely, defects with high formation energies are difficult to be incorporated and defects with lower formation energies are more likely to form.

III. RESULTS AND DISCUSSION

A. Structural properties of the anatase TiO_2

TiO_2 is a highly ionic semiconductor. The strength of the Coulombic attraction between the cation and anion is decisive in determining its crystal stability. In general, an ionic crystal prefers structures that maximize the number of oppositely charged nearest neighbors for each ion. This is in contrast to covalent semiconductors, which often exhibit tetrahedral bonding configurations that allow the formation of sp^3 hybridization. In TiO_2, the Ti atom (with a high oxidation number of +4) prefers to have a large number of O neighbors (oxidation number=−2), and strongly repels its Ti next-nearest neighbors. The specific geometry of the anatase crystal structure is such that each Ti atom has six O neighbors but only four Ti next-nearest neighbors. This explains why it is one of the stable crystal structures for TiO_2. Since O has a smaller oxidation number than Ti, it also has a smaller number (only three) of Ti neighbors. An illustration of the anatase crystal structure is shown in Fig. 2(a). One can think of this crystal structure as obtained from a distorted NaCl structure of TiO by removing half of the Ti atoms. The slight distortion from the ideal NaCl structure results in shorter Ti-O distances and longer Ti-Ti distances to further reduce the Madelung energy.

B. Formation energies and charge states of the native defects

Figure 2 shows the calculated atomic structures of Ti_i, V_{Ti}, $(O_2)_O$, and V_O. The defect formation energies are tabulated in Table I, as well as plotted as a function of the electron Fermi energy in Fig. 3. The most important feature of Fig. 3 is that none of the defects introduce any defect levels inside the band gap. The charge state of Ti_i, V_{Ti}, $(O_2)_O$, and V_O is 4+, 4−, 0, and 2+, respectively.[20] Moving the Fermi level across the band gap cannot change the charge state of these defects. Even if the Fermi level is moved into the valence or conduction band, there is still no significant filling of the defect, because the defect-induced electronic states are all delocalized resonant states, as revealed by the partial DOS in Fig. 4.[21] As a result, none of these defects is a carrier trap.

Due to the well-known LDA gap problems, our calculated conduction-band minimum at the special k-points (ε_k) used for the Brillouin zone integration, indicated in Fig. 3 by the dashed line, is smaller than the experimental gap. However, the defect states shown in Fig. 4 are not expected to fall into the band gap when a band-gap correction is applied, because they are all delocalized resonant states with symmetries resembling those of the extended band states (i.e., both the donors [Ti_i and V_O] and conduction-band edge states have the Ti d character, while both the acceptors [$(O_2)_O$ and V_{Ti}] and valence-band edge states have the O p character), which should follow the band edge closely in schemes that correct the LDA band gap. In this regard, a GW quasiparticle calculation like the one in Ref. 22 is highly desirable to confirm such predictions.

Being free of native-defect-induced gap states is a result of high ionicity of the TiO_2. The Ti has a small electronega-

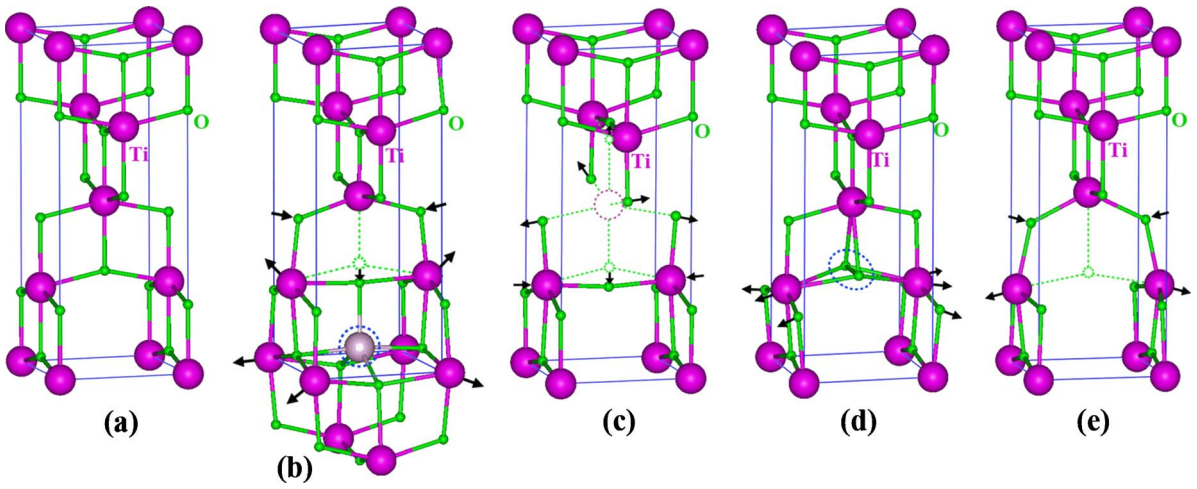

FIG. 2. (Color online) Atomic structures of (a) bulk anatase TiO_2, (b) Ti_i^{4+}, (c) V_{Ti}^{4-}, (d) $(O_2)_O$, and (e) V_O^{2+} defects. The large spheres are the Ti atoms and the small spheres are the O atoms. Relaxation directions of neighboring atoms are selectively indicated by the arrows. In some cases, ideal positions of the atoms before relaxation or removal are shown by dashed circles.

tivity (Ti=1.54 in Pauling scale), smaller than the cations in all major group IV, III-V, and II-V semiconductors, and the O has a very large electronegativity of 3.44. The defect states for Ti_i and V_O are the Ti *d* states. Figures 4(b) and 4(e) show that these states are all above the CBM. In fact, a nominal Ti ion also has levels above the CBM. These explain why Ti_i and V_O do not induce gap levels and, as a matter of course, the large heat of formation of TiO_2 (−10.25 eV, see Sec. II). Also due to the strong electron donating tendency of Ti, the O atoms around a V_{Ti} can easily draw electrons, resulting in defect states below the VBM.

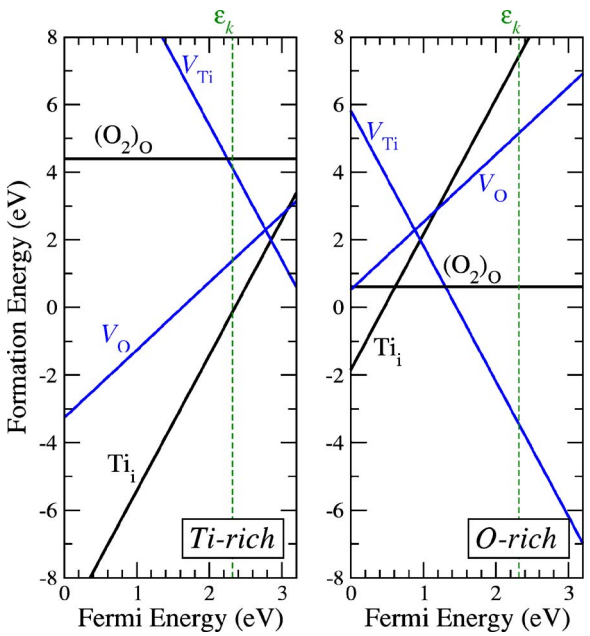

FIG. 3. (Color online) Defect formation energies as a function of the Fermi level, under the Ti-rich (left panel) and O-rich (right panel) growth conditions, respectively. The slope of the line is an indication of the charge state of the defect. The Fermi energy, referenced to the top of the valence band, is all the way to the experimental band gap. The vertical dotted line is the calculated band gap at the special *k*-point.

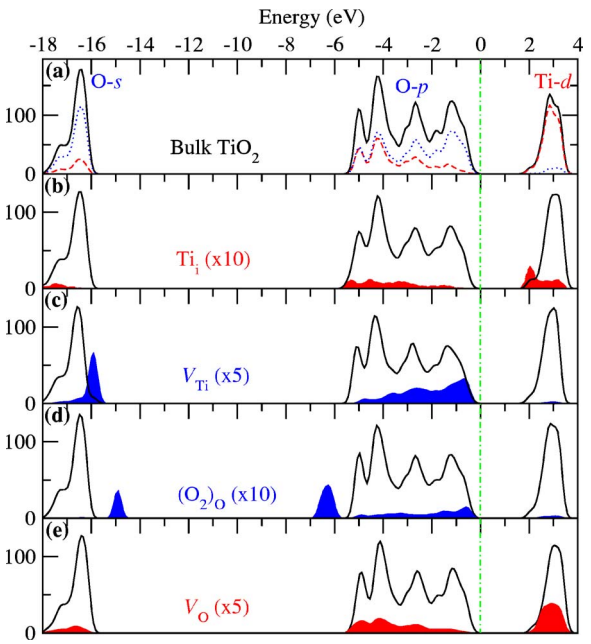

FIG. 4. (Color online) Site decomposed electron density of states (DOS). For each atom center, the local partial DOS in a sphere radius *R* (Ti:*R*=1.48 Å and O:*R*=0.74 Å) is calculated. (a) Bulk TiO_2, where the solid line is the total DOS, the dashed line is the DOS on Ti, and the dotted line is the DOS on O. (b)–(e) Native defects where the shaded area is the DOS on the atoms directly related to the defect (scaled up by a factor given in parentheses for clarity) and the solid line is the DOS on the remaining atoms in the supercell. Vertical dash-dotted line indicates the position of the VBM.

C. Structure and stability of the native defects

1. Titanium interstitial (Ti_i)

Titanium interstitial favors an octahedral site [Fig. 2(b)]. The site is similar to a lattice Ti site in that horizontally there are four neighboring O atoms nearly in a plane. The main difference is that the lattice Ti site also has two additional O atoms (one located directly above and one below). However, when a Ti is placed on the octahedral interstitial site, as shown in Fig. 2(b), one of the vertical O neighbors moves considerably toward it. The surrounding Ti atoms are also slightly relaxed outward, due to the electrostatic repulsion between positively charge Ti ions.

Ti_i is a *quadruple shallow donor*. Under the Ti-rich and *p*-type condition, i.e., E_F is at the VBM, which is the extremely favorable situation for Ti_i^{4+} incorporation, the formation energy of the Ti_i is negative and, surprisingly, very low, i.e., −9.42 eV. This low formation energy is due mainly to the energy gain from a transfer of four electrons to the low E_F level. In addition, the anatase structure contains a lot of open space that can accommodate the interstitial atom without much strain. (First-principles studies of SnO_2 also found Sn_i^{4+} to have a negative formation energy at the cation-rich and *p*-type condition.[23]) This Ti_i formation energy remains negative as long as $E_F < 2.4$ eV (Fig. 3, left panel). A negative formation energy means that the formation of the defect is spontaneous, so it is impossible to grow TiO_2 under such conditions. (Even if one begins in the *p*-type region, the rapid formation of the quadruple donor Ti_i would quickly turn the sample *n*-type.) Under the O-rich condition, Ti_i may also have a negative formation energy unless $E_F > 0.5$ eV (see Fig. 3, right panel). From these results, we expect it to be difficult to dope TiO_2 *p*-type under any equilibrium growth conditions.

The low formation energy of Ti_i makes it the strongest candidate for the shallow donors observed in undoped anatase TiO_2 with high purity.[24] The low formation energy may also explain the earlier observations of Ti_i in oxygen-deficient rutile samples by ion beam channeling,[25] electron paramagnetic experiment,[26] and others as summarized in the review in Ref. 27. Although most of the experimental works were performed on rutile TiO_2, the local structures of rutile and anatase are very similar. Because the oxygen-deficient TiO_2 samples were prepared by heating TiO_2 (1000–1400 °C) in a reducing atmosphere for a prolonged period of time (typically 100–1000 h), it is likely that some of the O atoms first migrate out of the sample, leaving vacancies behind. However, due to the small formation energy of Ti_i, these oxygen vacancies will subsequently react with the remaining TiO_2 via the following reaction:

$$m\mathrm{TiO_2} + 2nV_{\mathrm{O}}^{2+} \rightarrow (m-n)\mathrm{TiO_2} + n\mathrm{Ti}_i^{4+} + 2ne^-, \qquad (5)$$

to produce Ti_i interstitials.

2. Titanium vacancy (V_{Ti})

The atomic structure of V_{Ti} is shown in Fig. 2(c). As one Ti atom is missing here, the surrounding O atoms relax outward, each to a point approximately halfway between its two remaining Ti neighbors. This relaxation increases the Coulomb binding by reducing the Ti-O distances while increasing the O-O distances.

The Ti vacancy is a *quadruple shallow acceptor*. Under the O-rich (i.e., Ti-poor) growth condition, the formation energy of V_{Ti} is negative if $E_F > 1.46$ eV. This means that V_{Ti} will spontaneously form and, as a result (and because V_{Ti} is a quadruple acceptor), E_F will be pushed down until it is below 1.46 eV. Under the Ti-rich condition, V_{Ti} is still a low-energy defect, and hence acts as a leading native acceptor. To the best of our knowledge, there is still no experimental identification of the V_{Ti}.

3. Oxygen interstitial (O_i)

Isolated interstitial O has high formation energy and is hence unstable. It spontaneously binds with an O on the lattice site, forming a substitutional O_2 molecule, $(O_2)_O$. Each lattice O atom has an oxidation number of −2. A neutral $(O_2)_O$ thus contains two more electrons compared to a free O_2 molecule in the vacuum. Similar to the case of substitutional diatomic molecules in ZnO,[4] the additional two electrons occupy and completely fill the molecular $pp\pi^*$ states, which lie below the VBM. The atomic structure of the $(O_2)_O$ is shown in Fig. 2(d). Because the charge neutral O_2 is electrostatically equivalent to any O atom on a lattice site, one can expect that there should not be any large relaxation of the neighboring atoms. All the neighboring Ti atoms relax only slightly outward. Substitutional O_2 has a bond length of 1.46 Å, which is very similar to substitutional O_2 in ZnO [also 1.46 Å (Ref. 4)]. The bond length of a substitutional O_2 is longer than that of a free O_2 [1.21 Å (Ref. 28)] due mainly to the occupation of the two extra electrons on the $pp\pi^*$ *antibonding* orbital, and to the screening effect of the host. Under the Ti-rich condition, the $(O_2)_O$ has high formation energy and is hence unlikely to exist in any appreciable amount. However, under the O-rich condition, its formation energy is reasonably low, making it an important defect.

4. Oxygen vacancy (V_O)

For O vacancy, each of the three nearest-neighbor Ti atoms moves away from the vacancy toward its five remaining O neighbors, as illustrated in Fig. 2(e). The next-nearest-neighbor O atoms move slightly inward due to the absence of electrostatic repulsion by the missing O atom.

Our calculations show that V_O is a *double donor*. This is because the O has an oxidation state 2- or, in other words, has two additional electrons transferred from the three surrounding Ti atoms. When the oxygen is removed as a neutral atom, the two additional electrons are no longer needed, making the V_O a double donor. This is consistent with first-principles calculations by Sullivan and Erwin.[29] The formation energy of the V_O reported in Ref. 29 is slightly higher than ours, partly because they used the "Makov-Payne correction."[19]

Our calculation suggests that V_O is *not* a dominant native defect *near equilibrium growth* conditions. Even in the Ti-rich growth condition, which is most favorable for V_O formation, Ti_i has a lower formation energy than V_O at all possible E_F. However, V_O can be created in certain processes

such as annealing to create oxygen-deficient samples. Although the energetics suggests that subsequent conversion to Ti_i via Eq. (5) is likely, the kinetics may not support such a process, as one only needs to break the Coulomb bindings with three neighboring Ti to free an O, but six such bindings to free a Ti. This might be why V_O are still observed by certain experiments (thermogravimetric, electrochemical titration, diffusion, and conductivity measurements as discussed in Ref. 27).

IV. CONCLUSION

Our calculations of native defects in anatase TiO_2 provide detailed information on the atomic structures and electronic properties for each of them. We found that Ti_i is a quadruple donor with very low formation energy, especially in *p*-type samples but also in *n*-type samples. This makes it the strongest candidate responsible for the native *n*-type conductivity observed in TiO_2. While V_O has higher formation energy than that of Ti_i, the kinetic barrier for creating V_O from a perfect TiO_2 is expected to be lower than that for creating Ti_i. Hence, post-growth formation of V_O is also possible, especially after the sample has been heated for a prolonged time. A quadruple acceptor V_{Ti} is the lowest-energy acceptor in TiO_2. Thus in undoped samples, Ti_i and V_{Ti} should be the leading donor and acceptor, respectively. Formation of Ti_i is further enhanced under the Ti-rich growth condition, while that of V_{Ti} is further enhanced under the O-rich growth condition. Interstitial oxygen would spontaneously bond to lattice oxygen, forming electrically inactive O_2 dimer substituting on one O lattice site. Antisite defects have relatively high formation energies and are likely to spontaneously break into isolated vacancies and interstitials. Our calculations also show that none of the four low-energy defects, Ti_i, O_i, V_{Ti}, and V_O, introduce any defect levels inside the DFT band gap.

ACKNOWLEDGMENTS

This work was supported by the National Synchrotron Research Center (Thailand) under Contract No. 2547/004. The work at NREL was supported by the U.S. DOE under Contract No. DE-AC36-99GO10337. We acknowledge R. Thongpool for bringing the problem of defects in TiO_2 to our attention. We also thank P. Reunchan and S. Jungthawan for their help with some of the calculations and S. Rujirawat and N. Kopidakis for fruitful discussions.

[1] M. R. Hoffmann, S. T. Martin, W. Choi, and D. W. Bahnemann, Chem. Rev. (Washington, D.C.) **95**, 69 (1995) and references therein.
[2] J. C. Yu, J. Yu, W. Ho, Z. Jiang, and L. Zhang, Chem. Mater. **14**, 3808 (2002).
[3] Q. Chen and H.-H. Cao, THEOCHEM **723**, 135 (2005).
[4] S. Limpijumnong, X. Li, S.-H. Wei, and S. B. Zhang, Appl. Phys. Lett. **86**, 211910 (2005).
[5] S. Limpijumnong and C. G. Van de Walle, Phys. Rev. B **69**, 035207 (2004).
[6] J. Neugebauer and C. G. Van de Walle, Phys. Rev. B **50**, R8067 (1994).
[7] S. Limpijumnong, S. B. Zhang, S.-H. Wei, and C. H. Park, Phys. Rev. Lett. **92**, 155504 (2004); A. F. Kohan, G. Ceder, D. Morgan, and C. G. Van de Walle, Phys. Rev. B **61**, 15019 (2000).
[8] D. Vanderbilt, Phys. Rev. B **41**, R7892 (1990).
[9] G. Kresse and J. Furthmüller, Comput. Mater. Sci. **6**, 15 (1996).
[10] C. J. Howard, T. M. Sabine, and F. Dickson, Acta Crystallogr., Sect. B: Struct. Sci. **47**, 462 (1991).
[11] A. Fahmi, C. Minot, B. Silvi, and M. Causá, Phys. Rev. B **47**, 11717 (1993).
[12] R. Asahi, Y. Taga, W. Mannstadt, and A. J. Freeman, Phys. Rev. B **61**, 7459 (2000).
[13] M. Calatayud, P. Mori-Sánchez, A. Beltrán, A. M. Pendás, E. Francisco, J. Andrés, and J. M. Recio, Phys. Rev. B **64**, 184113 (2001).
[14] S. B. Zhang and J. E. Northrup, Phys. Rev. Lett. **67**, 2339 (1991); J. E. Northrup and S. B. Zhang, Phys. Rev. B **50**, 4962 (1994).
[15] S. B. Zhang, S.-H. Wei, and A. Zunger, Phys. Rev. B **63**, 075205 (2001).
[16] S. B. Zhang, J. Phys.: Condens. Matter **14**, R881 (2002).
[17] H. Tang, H. Berger, P. E. Schmid, F. Lévy, and G. Burri, Solid State Commun. **23**, 161 (1977).
[18] R. A. Parker, Phys. Rev. **124**, 1719 (1961).
[19] G. Makov and M. C. Payne, Phys. Rev. B **51**, 4014 (1995).
[20] The reported stable charge states of +1 and 0 for V_O [J. M. Sullivan and S. C. Erwin, Phys. Rev. B **67**, 144415 (2003)] are probably due to electron filling of the conduction-band edge states rather than the actual defect states, because their calculated transition levels are >2.6 eV above the VBM and are hence above our calculated CBM (they have used a very similar calculation method to ours).
[21] For vacancies, the defect atoms include the nearest neighbors of the missing atom, i.e., six O atoms for V_{Ti} and three Ti atoms for V_O. For Ti_i, only the interstitial Ti atom itself is included as the defect atoms, whereas for $(O_2)_O$, both O atoms in the dimer are included.
[22] S. B. Zhang, D. Tománek, M. L. Cohen, S. G. Louie, and M. S. Hybertsen, Phys. Rev. B **40**, 3162 (1989).
[23] C. Kiliç and A. Zunger, Phys. Rev. Lett. **88**, 095501 (2002).
[24] L. Forro, O. Chauvet, D. Emin, L. Zuppiroli, H. Berger, and F. Lévy, J. Appl. Phys. **75**, 633 (1994).
[25] E. Yaki, A. Koyama, H. Sakairi, and R. R. Hasiguti, J. Phys. Soc. Jpn. **42**, 939 (1977).
[26] M. Aono and R. R. Hasiguti, Phys. Rev. B **48**, 12406 (1993); R. R. Hasiguti and E. Yagi, *ibid.* **49**, 7251 (1994).
[27] J. Sasaki, N. L. Peterson, and K. Hoshino, J. Phys. Chem. Solids **46**, 1267 (1985), and references therein.
[28] K. P. Huber and G. Herzberg, *Molecular Spectra and Molecular Structure. IV. Constants of Diatomic Molecules* (Van Nostrand Reinhold, New York, 1979).
[29] J. M. Sullivan and S. C. Erwin, Phys. Rev. B **67**, 144415 (2003).